Iodination of Single-Walled Carbon Nanotubes

ARTICLE *in* CHEMISTRY OF MATERIALS · JANUARY 2008

Impact Factor: 8.35 · DOI: 10.1021/cm062730x

Available online at www.sciencedirect.com
ScienceDirect
Carbon 45 (2007) 2744–2750
CARBON
www.elsevier.com/locate/carbon

A photoelectron spectroscopy study of ion-irradiation induced defects in single-wall carbon nanotubes

Amit K. Chakraborty [a,b], R.A.J. Woolley [b], Yu.V. Butenko [c], V.R. Dhanak [d], L. Šiller [c], M.R.C. Hunt [a,*]

[a] Department of Physics, University of Durham, Durham, DH1 3LE, UK
[b] School of Physics and Astronomy, University of Nottingham, University Park, Nottingham, NG7 2RD, UK
[c] School of Chemical Engineering and Advanced Materials, University of Newcastle upon Tyne, Newcastle upon Tyne, NE1 7RU, UK
[d] Physics Department, University of Liverpool, Liverpool L69 3BX, UK

Received 16 August 2006; accepted 18 September 2007
Available online 22 September 2007

Abstract

Valence band and core level photoemission spectroscopies were used to study the changes brought about by irradiation of a single-wall carbon nanotube (SWCNT) film by 3 keV Ar^+ ions at room temperature. At low ion doses (low defect density) an increase in spectral intensity near the Fermi level (E_F) is observed, associated with formation of localized defect-related states. These states are acceptor-like as evidenced by a shift to lower binding energy for both valence band features and the C1s core level. For large ion doses (high defect density) the spectral intensity near E_F decreases, valence band features associated with delocalized π bonding disappear, and a core level component associated with sp^3 bound carbon appears. This behaviour is attributed to amorphisation of the SWCNT films and occurs at ion doses consistent with those theoretically predicted.

1. Introduction

Energetic particles such as electrons [1–7], protons [8], and atomic ions [9–24] can be used to create artificial defects in carbon nanotubes (CNTs), enabling the influence of such imperfections on nanotube physical properties to be examined. Consequently, numerous studies, both experimental and theoretical, have appeared in the literature on irradiation of CNTs. These studies have revealed structural modification such as bending, folding, kinking, radial deformation, shrinkage of diameter, coalescence and cutting of nanotubes [1–3,8] modification of electronic transport and field emission [4,5,10–14] properties, and amorphisation of both single-wall CNTs and multi-wall carbon nanotubes (MWCNTs) [8,15,16]. A range of potential applications of irradiation such as the creation of nanotube inter-molecular junctions [6,7,17,18] through 'welding' by electron or ion-irradiation have been explored.

Although several authors have theoretically investigated the effects of inert ion-irradiation on single-wall carbon nanotubes (SWCNTs) [17–25], a limited number of experimental studies on ion-irradiation induced defects in CNTs have been reported, the majority focusing on MWCNTs. For example, Zhu et al. [15] irradiated MWCNTs with 3 keV Ar^+ ions and employed X-ray photoelectron spectroscopy (XPS) and transmission electron microscopy (TEM) to study the result. A complete transformation of MWCNTs into amorphous carbon nanorods was observed together with the apparent observation of 'dangling bonds' in valence band spectra. Brzhezinskaya et al. [16] reported disruption of delocalized π bonding within MWCNTs when subjected to Ar^+ ion-irradiation, due to creation of defects. However, a detailed spectroscopic study of the results of inert ion-irradiation on the physical properties of SWCNTs remains lacking. In this article we investigate

* Corresponding author. Fax: +44 191 3345823.
E-mail address: m.r.c.hunt@durham.ac.uk (M.R.C. Hunt).

0008-6223/$ - see front matter © 2007 Elsevier Ltd. All rights reserved.
doi:10.1016/j.carbon.2007.09.036

the effects of artificially-induced defects produced by Ar^+ ion-irradiation on the electronic and atomic structure of SWCNTs as a function of ion fluence (dose) using valence band and core level photoemission spectroscopies.

2. Experiment

XPS and valence band photoemission spectroscopy were performed at Beamline 4.1 of the Synchrotron Radiation Source (SRS), Daresbury, UK. Purified SWCNTs produced by the HiPCO method (Carbon Nanotechnologies Inc.) were dispersed in 2-propanol by gentle ultrasonication in a conventional ultrasonic cleaning bath to make a uniform suspension. The use of vigorous sonication and surfactants was avoided due to the associated sample contamination, which is extremely difficult to remove [26]. Drops of this suspension were then deposited onto silicon (100) substrates (with a native oxide layer) to create a "thick" film (visible by eye) which suppressed all photoemission signal from the underlying substrate. The resulting samples were mounted on a sample holder between two tantalum clips which made good electrical contact to the nanotube film. These samples were immediately loaded into an ultra high vacuum (UHV) chamber (base pressure less than 1×10^{-10} Torr). Samples were outgassed overnight and then annealed at 800 °C, while maintaining a chamber pressure less than 5×10^{-9} Torr, for at least one hour in order to desorb any residual organic solvents, oxygen-containing surface groups, and any water trapped in the sample. Maximum annealing temperatures were limited to 1000 °C – for extended anneals significantly above this temperature silicon was observed to diffuse upwards through the film and react with the carbon nanotubes. All the spectra presented here were measured at room temperature after allowing the samples to cool sufficiently.

After cleaning and characterisation, samples were irradiated by an argon ion beam produced by a field ion source at an Ar pressure of up to 1.2×10^{-5} Torr. The purity of the Ar gas was monitored by a quadrupole mass spectrometer. A constant beam energy of 3 keV was used in all cases, while sample current was varied between 3.0 μA and 30 μA. The total ion dose was estimated from the integrated sample current. Several irradiation doses were given to each sample and corresponding spectra were acquired after each dose. A number of samples were studied to ensure reproducibility, and samples were at room temperature during ion-irradiation.

Photoemission spectra were acquired *in situ* with a SCIENTA SES-200 hemispherical analyzer using 1253.6 eV photons from a conventional $Mg K_\alpha$ X-ray source for core level photoelectron spectra (XPS) and 55 eV photons from the Synchrotron source for valence band spectroscopy. All spectra were acquired in normal emission geometry. Binding energies were calibrated by the position of the Fermi cut-off of a gold foil in electrical contact with the sample for valence band data, and by the position of the Au $4f_{7/2}$ line (84.0 eV) in the case of core level data. Likewise, the energy resolution was derived from the width of the Fermi cut-off in the case of valence band data and by the width of Au $4f_{7/2}$ line in core level data; values of ~0.2 eV and ~0.8 eV were measured, respectively. All data presented here are normalised with respect to total integrated peak area.

The cleanliness of the samples was thoroughly evaluated with XPS and monitored throughout the experiment. After cleaning no contamination was detectable at the noise level of our experiment. In order to further evaluate our samples extensive *ex-situ* characterisation of material from the same batch, deposited on to oxidised silicon in the same manner, was undertaken using monochromated XPS, Raman spectroscopy, and atomic force microscopy (AFM) – to be reported in detail elsewhere. The high resolution XPS measurements, performed on as-introduced (non-annealed) samples, showed the presence of trace quantities of iron (~0.8 at.%), primarily in the form of oxide, which originates from residual catalyst used in SWCNT growth, oxygen (~8 at.%) and carbon. No other elements could be detected above the sensitivity threshold of the XPS measurement (better than 0.1 at.%). Raman spectra had a large ratio of G band to D band intensity, indicating a high degree of graphitisation and low defect density. AFM studies did not detect the presence of amorphous carbon or graphitic particles.

3. Results and discussion

Fig. 1 shows a plot of valence band spectra from an ion-irradiated SWCNT film as a function of ion dose. Two prominent peaks are observed in the valence band of the pristine (zero ion dose) sample, located at binding energies of 3.0 ± 0.1 eV and 7.8 ± 0.1 eV. The peak at 3.0 eV in the spectrum of the undamaged film arises from states associated with conjugated π bonds within the SWCNTs and that at 7.8 eV, the maximum of the 'graphitic' valence band, is due to σ bonding states [27,28]. Peaks at approximately 4 and 6.5 eV arise from population of mixed π and σ states [27]. The inset to Fig. 1 shows the area under the main peak associated with π bonding (shaded region in the top spectrum) which is characteristic of graphitic materials. It is evident that the π peak rapidly decreases with increasing ion dose. The rapid destruction of the π bonding network within the nanotubes we observe is consistent with the data of Brzhezinskaya et al. [16] who observed a decrease of the energy of the π plasmon in electron energy loss spectra obtained from MWCNTs irradiated with 1 keV Ar^+ ions.

Upon ion-irradiation we observe (Fig. 1) that both the π and σ bonding peaks initially shift to lower binding energy. The maximum of the σ peak, which is initially at a binding energy of 7.8 eV, shifts to 7.4 ± 0.1 eV after an ion dose of 210 μC (~1.3×10^{15} ions/cm^2). The shift to lower binding energy for the peak associated with π states is smaller (approximately 0.1 eV) and is harder to quantify due to the broadening of the peak and changes to the background. For ion doses above 210 μC the broad valence band fea-

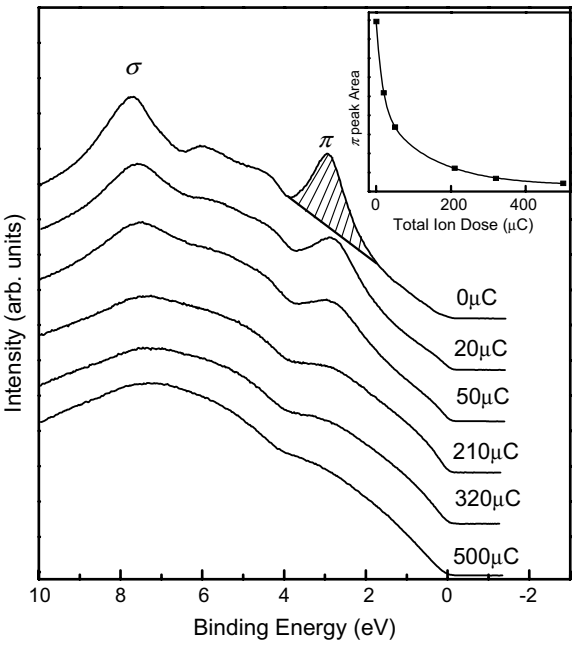

Fig. 1. Evolution of the valence band of a SWCNT film as a function of Ar^+ ion dose. The shaded region in the top spectrum represents the area under the main peak associated with π-bonding. The inset shows the π-peak area, as a function of ion dose, in which the solid line is a guide to the eye.

tures change little. The broadening of the valence band spectra can be attributed to increased disorder within the nanotube films, as expected from the random incorporation of defects, which has the greatest impact on the π bonding network. We find no evidence of the 'dangling bonds' reported by Zhu et al. [15] (sharp features at 9.6 eV and 22.6 eV binding energy) in the valence band of ion irradiated MWCNTs and C_{60}, even at the highest ion doses reported here. In a study of Ar^+ ion-irradiation of C_{60} thin films, in which partial destruction of the fullerene cages was observed, Reinke and Oelhafen [29] also failed to observe any 'dangling bond' related features. A similar feature to the lower energy 'dangling bond' peak reported in the work of Zhu et al. [15] was reported in a study of Ar^+ ion irradiation of amorphous carbon by Reinke et al. [30] but this peak was attributed to Ar 3p emission associated with Ar trapped within the film during irradiation and not to dangling bonds.

Further confirmation of the absence of a substantial concentration of dangling bonds in the ion irradiated SWCNT films is provided by exposure to ambient atmosphere, performed within two hours of initial irradiation. In Fig. 2 we plot C1s core level photoemission spectra obtained from an ion-irradiated SWCNT film before (solid line) and after the film was exposed to atmosphere for 5 min (hollow circles). The absence of any detectable change in lineshape upon exposure of irradiated SWCNTs to the ambient indicates a remarkable lack of reactivity. It can therefore be inferred that dangling bonds, which are created by ion bombardment due to atom removals and are highly reactive, cannot be available for reaction with atmospheric gases at a detectable concentration.

Both metastable monovacancy structures [23] and the generally accepted isolated monovacancy ground state, the so-called '5-1db' (pentagon plus one dangling bond) structure [31,32] have dangling bonds associated with them. The absence of any changes in the C1s photoemission spectra after exposure to ambient atmosphere suggests that the dangling bonds formed by initial ion-irradiation were somehow satisfied in the ultra-high vacuum ambient prior to exposure to atmosphere. The absence of any time-dependence in our data indicates that this saturation occurred rapidly. The simplest vacancy structure which can lead to elimination of dangling bonds is the divacancy. Theoretical work [23] shows that, at the irradiation energies employed in this study, around half of the defects created by ion-irradiation should be in the form of vacancy clusters (including divacancies), the rest existing as isolated monovacancies. It has been shown that the migration barrier for a 5-1db defect is relatively small (~1 eV) [33], allowing the monvacancies present to diffuse and form (immobile) divacancies at modest temperatures, eliminating dangling bonds. Saturation of dangling bonds through chemisorption of residual gases in the ultra high vacuum environment is also a distinct possibility. In a recent theoretical study Lu and Pan [34] showed that 5-1db defects were highly reactive towards both atomic and molecular hydrogen. Indeed, for atomic hydrogen there was found to be no activation barrier for saturation of the 5-1db dangling bond. Since atomic and molecular hydrogen constituted the majority of the residual gas in our vacuum chamber it is likely that this species would dominate chemosorption-induced saturation of dangling bonds. Saturation of dangling bonds with hydrogen is also consistent with the absence of any contamination observed during our experiment – hydrogen cannot be detected by XPS.

In Fig. 3, we present valence band spectra of the region in close proximity to the Fermi level, obtained at higher energy resolution and with better signal-to-noise than the data shown in Fig. 1. Fig. 3 demonstrates that this region

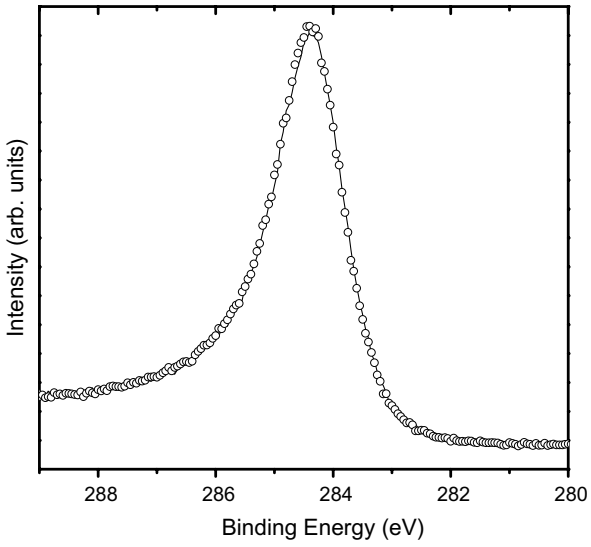

Fig. 2. C1s photoemission spectra from SWCNT film irradiated to a dose of 500 μC (solid line) and subsequently exposed to atmosphere (circles). Both width and position of the C1s line remain unchanged after air exposure.

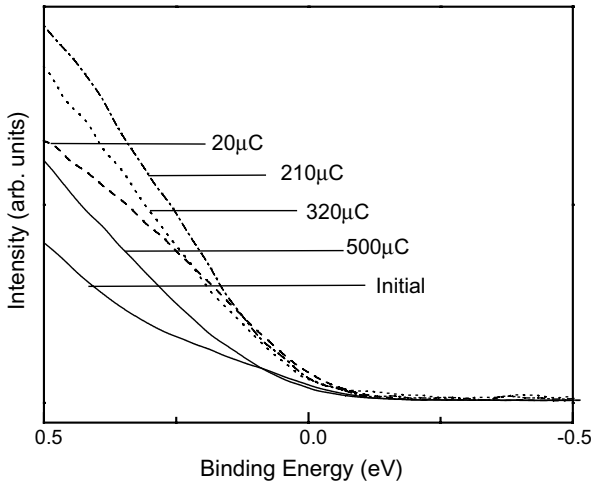

Fig. 3. Evolution of the valence band photoemission spectra close to the Fermi level, measured as a function of ion dose. The spectra were obtained under the same conditions as those of Fig. 1, but with better resolution and signal-to-noise ratio.

initially shows an increase in intensity (hence density of states – DOS) upon irradiation. Spectral changes near to the Fermi level are consistent with a redistribution of DOS associated with the theoretically predicted formation of localized electronic states in the presence of point defects such as vacancies, substitutional impurities, topological defects [35,36] unsaturated [31] and saturated 5-1db defects [37]. Even when the primary change induced by the defect is an acceptor state located above the Fermi level (and hence inaccessible to photoemission spectroscopy), such as in the case of an unsaturated 5-1db defect [31], a rearrangement of the *occupied* density of states near the Fermi level also occurs, consistent with our data. Studies involving ion-irradiation of graphitic materials have also shown a similar increase in the DOS at the Fermi level [28–30]. The absence of clear peak(s) in our data associated with localized states is likely to arise from the random distribution of defects within the SWCNT film, and the spread in diameter/chirality of the nanotubes in our sample. Hence we are unable to determine the precise nature of the defects formed by ion-irradiation.

Defect states can have a profound impact upon electronic transport properties of nanotubes [11,13,35,36,38–40]. Vacancies [5], including both unsaturated and saturated 5-1db structures [31,37], can produce acceptor-like states within graphitic materials, and the shift of valence band features to lower binding energy can be attributed to a shift of the Fermi level associated with 'hole doping' of the defective nanotubes. Reinke and Oelhafen [29] observed a similar shift of ~0.4 eV in both valence band and core level features when C_{60} fullerene was irradiated by low energy (500 eV) Ar^+ ions at doses comparable to those reported here. However, a decrease of spectral intensity close to E_F from its maximum is apparent in Fig. 3 at high ion doses (above 210 μC). As we shall discuss in more detail below, the high-dose variation is due to the onset of amorphisation of the SWCNT film.

Fig. 4 shows a plot of C1s spectra obtained from clean and ion irradiated SWCNT films. At all but the highest irradiation doses the spectrum can be fitted accurately with a single Doniac-Šunjić lineshape associated with sp^2 bound carbon, convolved with a Gaussian (representing instrumental and disorder induced broadening), and a Shirley background (Fig. 5a). The spectrum from the pristine sample shows a single peak at 284.42 ± 0.03eV with an asymmetry parameter, α, of 0.14, consistent with previous work [41]. Upon Ar^+ irradiation the C1s line immediately shifts to lower energy (Table 1) and this shift saturates, to within experimental error, at 0.13 ± 0.04 eV. The position of the

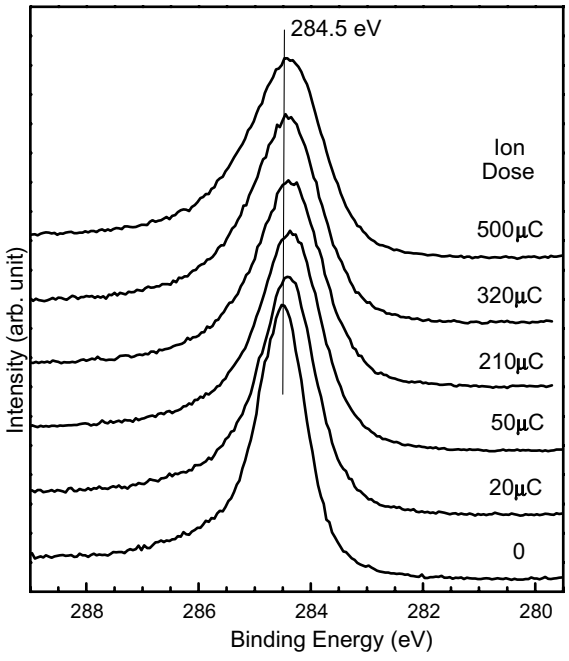

Fig. 4. Evolution of C1s core level photoemission spectra as a function of ion dose.

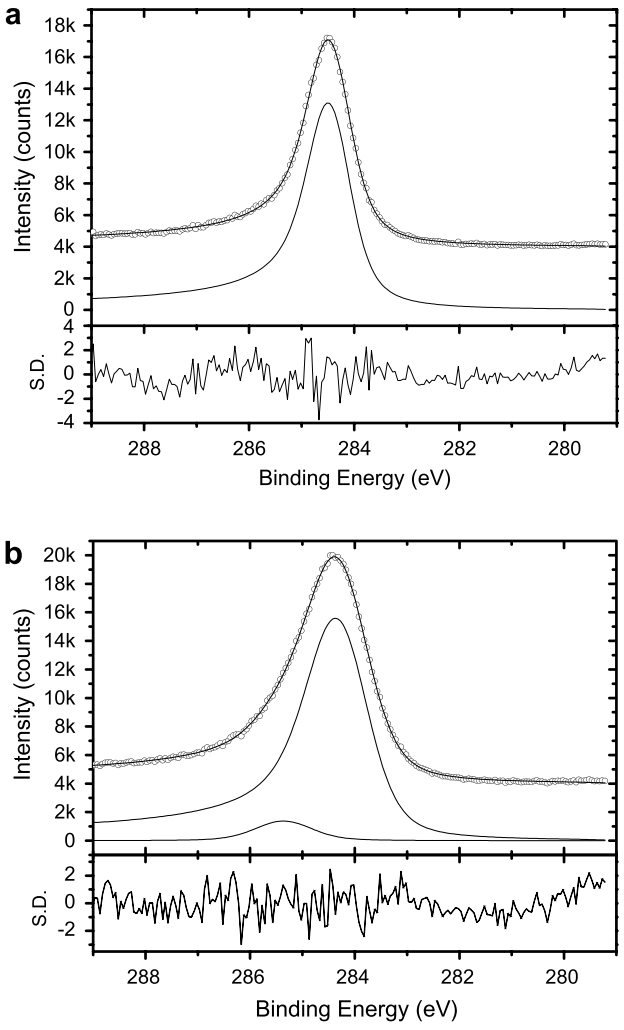

Fig. 5. C1s photoelectron spectra of (a) a pristine SWCNT film, (b) a SWCNT film subjected to 500 μC ion-irradiation. The hollow circles represent the experimental data, which is superimposed with a solid line representing the fit. Fit components (excluding the Shirley background) are also shown inside the experimental spectrum. The bottom panels depict the residuals from curve fitting (in units of standard deviation).

Table 1
List of fitting parameters used to decompose C1s spectra

Irradiation dose ($\mu C/cm^2$)	sp^2 Component (Doniac-Šunjić)	sp^3 Component (Gaussian–Lorentzian)
0	Binding energy (eV), 284.42 Asymmetry parameter, 0.14 FWHM (eV), 1.1 Fractional area (%), 100	Not present
20	Binding energy (eV), 284.33 Asymmetry parameter, 0.14 FWHM (eV), 1.2 Fractional area (%), 100	Not present
50	Binding energy (eV), 284.30 Asymmetry parameter, 0.15 FWHM (eV), 1.3 Fractional area (%), 100	Not present
210	Binding energy (eV), 284.29 Asymmetry parameter, 0.13 FWHM (eV), 1.4 Fractional area (%), 97.5	Binding energy (eV), 285.44 FWHM (eV), 1.3 Fractional area (%), 2.5
320	Binding energy (eV), 284.33 Asymmetry parameter, 0.13 FWHM (eV), 1.5 Fractional area (%), 95	Binding energy (eV), 285.39 FWHM (eV), 1.4 Fractional area (%), 5
500	Binding energy (eV), 284.29 Asymmetry parameter, 0.13 FWHM (eV), 1.5 Fractional area (%), 87	Binding energy (eV), 285.19 FWHM (eV) 1.6 Fractional area (%), 13

Binding energies are measured to a precision of 0.03 eV, asymmetry parameters have a precision of 0.01. The uncertainty on the full width at half maximum (FWHM) of fit peaks is 0.1 eV, and that on relative peak areas is 3%.

C1s peak associated with sp^2 bonding remains unchanged at higher ion doses, but at doses of 210 μC and above a second C1s component, a Gaussian–Lorentzian lineshape ~1 eV higher in binding energy, is required to obtain a satisfactory fit. This second component can be attributed to the presence of sp^3 bound carbon [42] and indicates the presence of substantial damage in the nanotube film. The sp^3 bound carbon content of the film increases with ion dose, reaching a value of 13% at an ion dose of 500 μC.

The appearance of a C1s component associated with sp^3 bound carbon at large ion doses can be understood in terms of the level of damage within the carbon nanotube bundles at a given ion dose. In their molecular dynamics study of ion impact on SWCNT bundles Salonen et al. [24] investigated the dependence of the number of 'co-ordination defects' (i.e., the number of carbon atoms without the optimum three neighbour co-ordination of a pristine nanotube wall) as a function of ion energy. It was found that, for heavy ions, the number of co-ordination defects per ion depended linearly on ion energy to at least 1 keV. We estimate, under the reasonable assumption that the number of co-ordination defects per incident ion continues to increase linearly as the incident ion energy increases, that for an Ar^+ dose of 210 μC ($\sim 1.3 \times 10^{15}$ ions/cm^2) at 3 keV nearly every carbon atom is at a co-ordination defect. In other words, at doses above 210 μC reported here the basic geometric structure of the carbon nanotubes begins to break down and the film becomes amorphous. This is consistent with the observed break up, partial amorphisation and partial loss of tubular shape of (10, 10) nanotubes in molecular dynamics simulations under Ar ion doses of 2×10^{15} ions/cm^2 (Ref. [17]). In recent work, Brzhezinskaya et al. [16] inferred amorphisation from the appearance of a shoulder at 278 eV kinetic energy in Auger spectra from a MWCNT film irradiated with 1 keV Ar^+ ions. This feature, and changes in the π plasmon energy and width, appears to saturate at ion doses above ~100 μC/cm^2, also consistent with our observations.

The appearance of an sp^3 component to the C1s line is coupled with a decrease in spectral intensity near E_F in the valence band spectra (Fig. 3). Studies of amorphous carbon [42,43] have shown that photoemission intensity near E_F decreases as the ratio between sp^2 and sp^3 bound carbon decreases. However, in sp^2 bound carbon an increasing defect density leads to an increase in intensity near E_F [44]. Therefore, at high ion doses the appearance of sp^3 carbon in the core level spectra is accompanied by an amorphous-carbon like response of the valence band spectra. This behaviour may be regarded as a signature for the destruction of the SWCNTs and formation of amorphous carbon. It must be noted that the fits to our C1s data show that only a fraction of the carbon atoms in the most heavily irradiated nanotube films are sp^3 hybridised (~13%). This small concentration of fourfold co-ordinated carbon atoms is in agreement with theoretical studies in the literature involving ion-irradiation of nanotubes [19,22]. At low ion doses behaviour is dominated by the formation of localized defects which results in a shift of Fermi level, causing both valence and core level features to shift to lower binding energy, and an increase in the valence band density of states close to the Fermi level.

In the work reported by Zhu et al. [15] on irradiation of MWCNT films, the C1s line position was observed to shift to higher binding energy upon irradiation of the films by 3 keV Ar^+ ions, contrary to our observation of a shift towards lower binding energy upon irradiation of SWCNTs. This apparent discrepancy can be readily understood from the above arguments regarding amorphisation. The minimum ion dose that may be inferred from Ref. [15] is more than a factor of five larger than the maximum ion dose reported in our work. Thus the damage caused by irradiation

of the MWCNTs performed by Zhu and co-workers is much higher than that reported here and therefore led to complete amorphisation of the nanotubes. Indeed, transmission electron microscope (TEM) images reported in Ref. [15] revealed that after irradiation nanotubes were converted into amorphous carbon nanorods. Hence, the upward shift of C1s binding energy reported in Ref. [15] is not inconsistent with our data but represents a regime in which amorphisation of the nanotubes occurs, rather than the introduction of defects in a structure which maintains overall integrity. In a C1s envelope consisting of unresolved sp^2 and sp^3 components, the position of the envelope will shift upwards in binding energy with an increasing concentration of sp^3 bound carbon [42]. Given the degree of amorphisation of the nanotube films at high doses, we emphasise that theoretical investigations dealing with isolated defects should be compared with photoelectron spectra obtained in the low dose rather than in the high dose regime.

4. Conclusions

We have employed both core level and valence band photoemission spectroscopy to examine the impact of artificially induced defects, produced by irradiation with 3 keV Ar^+ ions at room temperature, on SWCNT films. At low doses the defects produced by ion irradiation act as 'acceptor states' leading to a shift to lower binding energies of core and valence features. An increase in spectral intensity is observed in valence band spectra close to the Fermi level, associated with disorder-induced states. At high ion doses a component associated with sp^3 bound carbon is required to fit core level data. At these doses the valence band peak associated with delocalized π bonding is lost and spectral intensity near the Fermi level begins to fall. Taken together these phenomena indicate amorphisation of the SWCNT film, consistent with theoretical predictions at these ion doses. Irradiated SWCNT films do not show any evidence of chemical reactivity towards ambient atmosphere, which suggests that any dangling bonds produced by irradiation are rapidly saturated.

Acknowledgments

A.K.C. is grateful to the EPSRC and University of Nottingham for the award of a studentship. L.Š. acknowledges the Royal Society and EPSRC for financial support. We thank G. Miller for valuable technical support during the experiments. Yu.V.B. would like to thank the European Community's Sixth Framework Programme for award of a Marie Curie Incoming European Fellowship (MIF1-CT-2005-021528). This work was supported by CCLRC and EPSRC.

References

[1] Ajayan PM, Ravikumar V, Charlier J-C. Surface reconstructions and dimensional changes in single-walled carbon nanotubes. Phys Rev Lett 1998;81(7):1437–40.

[2] Kiang CH, Goddard III WA, Beyers R, Bethune DS. Structural modification of single-layer carbon nanotubes with an electron beam. J Phys Chem 1996;100(9):3749–52.

[3] Terrones M, Terrones H, Banhart F, Charlier J-C, Ajayan PM. Coalescence of single-walled carbon nanotubes. Science 2000;288(5469):1226–9.

[4] Miko C, Milas M, Seo JW, Couteau E, Barišić N, Gaal R, et al. Effect of electron irradiation on the electrical properties of fibers of aligned single-walled carbon nanotubes. Appl Phys Lett 2003;83(22):4622–4.

[5] Beuneu F, l'Huillier C, Salvetat J-P, Bonard J-M, Forro L. Modification of multiwall carbon nanotubes by electron irradiation: an ESR study. Phys Rev B 1999;59(8):5945–9.

[6] Jang I, Sinnott SB, Danailov D, Keblinski P. Molecular dynamics simulation study of carbon nanotube welding under electron beam irradiation. Nano Lett 2004;4(1):109–14.

[7] Terrones M, Banhart F, Grobert N, Charlier J-C, Terrones H, Ajayan PM. Molecular junctions by joining single-walled carbon nanotubes. Phys Rev Lett 2003;89(7):075505-1–4.

[8] Basiuk VA, Kobayashi K, Kaneko T, Negishi Y, Basiuk EV, Saniger-Blesa J-M. Irradiation of single-walled carbon nanotubes with high-energy protons. Nano Lett 2002;2(7):789–91.

[9] Wang ZX, Yu LP, Zhang W, Ding YF, Li YL, Han JG, et al. Amorphous molecular junctions produced by ion irradiation on carbon nanotubes. Phys Lett A 2004;324(4):321–5.

[10] Ahn KS, Kim JS, Kim CO, Hong JP. Non-reactive rf treatment of multiwall carbon nanotube with inert argon plasma for enhanced field emission. Carbon 2003;41(13):2481–5.

[11] Park JW, Kim J, Lee J-O, Kang KC, Kim J-J, Yoo K-H. Effects of artificial defects on the electrical transport of single-walled carbon nanotubes. Appl Phys Lett 2002;80(1):133–5.

[12] Suzuki M, Ishibashi K, Toratani K, Tsuya D, Aoyagi Y. Tunnel barrier formation using argon-ion irradiation and single quantum dots in multiwall carbon nanotubes. Appl Phys Lett 2002;81(12):2273–5.

[13] Kim D-H, Jang H-S, Kim C-D, Cho D-S, Kang H-D, Lee H-R. Enhancement of the field emission of carbon nanotubes straightened by application of argon ion irradiation. Chem Phys Lett 2003;378(3–4):232–7.

[14] Stahl H, Appenzeller J, Martel R, Avouris Ph, Lengeler B. Intertube coupling in ropes of single-wall carbon nanotubes. Phys Rev Lett 2000;85(24):5186–9.

[15] Zhu YF, Yi T, Zheng B, Cao LL. The interaction of C_{60} fullerene and carbon nanotube with Ar ion beam. Appl Surf Sci 1999;137(1–4):83–90.

[16] Brzhezinskaya MM, Baitinger EM, Shnitov VV. π-plasmons in ion-irradiated multiwall carbon nanotubes. Physica B 2004;348(1–4):95–100.

[17] Krasheninnikov AV, Nordlund K, Keinonen J, Banhart F. Ion-irradiation induced welding of carbon nanotubes. Phys Rev B 2002;66(24):1245403-1–5.

[18] Krasheninnikov AV, Nordlund K, Keinonen J, Banhart F. Making junctions between carbon nanotubes using an ion beam. Nucl Instrum Meth B 2003;202:224–9.

[19] Krasheninnikov AV, Nordlund K, Keinonen J. Carbon nanotubes as masks against ion irradiation: An insight from atomistic simulations. Appl Phys Lett 2002;81(6):1101–3.

[20] Krasheninnikov AV, Nordlund K. Stability of irradiation-induced point defects on walls of carbon nanotubes. J Vac Sci Tech B 2002;20(2):728–33.

[21] Krasheninnikov AV, Nordlund K, Keinonen J. Production of defects in supported carbon nanotubes under ion irradiation. Phys Rev B 2002;65(16):165423-1–8.

[22] Krasheninnikov AV, Nordlund K. Irradiation effects in carbon nanotubes. Nucl Instrum Meth B 2004;216:355–66.

[23] Krasheninnikov AV, Nordlund K, Sirivio M, Salonen E, Keinonen J. Formation of ion-irradiation-induced atomic-scale defects on walls of carbon nanotubes. Phys Rev Lett 2001;63(24):245405-1–6.

[24] Salonen E, Krasheninnikov AV, Nordlund K. Ion-irradiation induced defects in bundles of carbon nanotubes. Nucl Instrum Meth B 2002;193:603–8.
[25] Pomoell J, Krasheninnikov AV, Nordlund K, Keinonen J. Stopping of energetic ions in carbon nanotubes. Nucl Instrum Meth B 2003;206:18–21.
[26] Goldoni A, Petaccia L, Gregoratti L, Kaulich B, Barinov A, Lizzit S, et al. Spectroscopic characterization of contaminants and interaction with gases in single-walled carbon nanotubes. Carbon 2004;42(10):2099–122.
[27] Montalti M, Krishnamurthy S, Chao Y, Butenko YuV, Kuznetsov VL, Dhanak VR, et al. Photoemission spectroscopy of clean and potassium-intercalated carbon onions. Phys Rev B 2003;67(11): 113401-1–4.
[28] Schlogl R. Modification of the electronic structure of graphite by intercalation, chlorination and ion etching. Surf Sci 1987;189–190:861–72.
[29] Reinke P, Oelhafen P. Surface modification of C_{60} by ion irradiation studied with photoelectron spectroscopy. J Chem Phys 2002;116(22): 9850–5.
[30] Reinke P, Francz G, Oelhafen P, Ullmann J. Structural changes in diamond and amorphous carbon induced by low-energy ion irradiation. Phys Rev B 1996;54(10):7067–73.
[31] Lu AJ, Pan BC. Nature of single vacancy in achiral carbon nanotubes. Phys Rev Lett 2004;92(10):105504-1–4.
[32] Wang C, Wang CY. Geometry and electronic properties of single vacancies in achiral carbon nanotubes. Eur Phys J B 2006;54:243–7.
[33] Krasheninnikov AV, Lehtinen PO, Foster AS, Nieminen RM. Bending the rules: contrasting vacancy energetics and migration in graphite and carbon nanotubes. Chem Phys Lett 2006;418:132–6.
[34] Lu AJ, Pan BC. Interaction of hydrogen with vacancies in a (12, 0) carbon nanotube. Phys Rev B 2005;71(16):165416-1–6.
[35] Choi HJ, Ihm J, Louie SG, Cohen ML. Defects, quasibound states, and quantum conductance in metallic carbon nanotubes. Phys Rev Lett 2000;84(13):2917–20.
[36] Kostyrko T, Bartkowiak M, Mahan GD. Localization in carbon nanotubes within a tight-binding model. Phys Rev B 1999;60(15): 10735–8.
[37] Wang C, Zhou G, Wu J, Gu BL, Duan W. Effects of vacancy-carboxyl pair functionalization on electronic properties of carbon nanotubes. Appl Phys Lett 2006;89(17):173130-1–3.
[38] Hansson A, Paulsson M, Stafström S. Effect of bending and vacancies on the conductance of carbon nanotubes. Phys Rev B 2000;62(11): 7639–44.
[39] Anantram MP, Govindan TR. Conductance of carbon nanotubes with disorder: a numerical study. Phys Rev B 1998;58(8): 4882–7.
[40] Kong J, Yenilmez E, Tombler TW, Kim W, Dai HJ, Laughlin RB, et al. Quantum interference and ballistic transmission in nanotube electron waveguides. Phys Rev Lett 2001;87(10):106801-1–4.
[41] Goldoni A, Larciprete R, Gregoratti L, Kaulich B, Kiskinova M, Zhang Y, et al. X-ray photoelectron microscopy of the C1s core level of free-standing single-wall carbon nanotube bundles. Appl Phys Lett 2002;80(12):2165–7.
[42] Díaz J, Paolicelli G, Ferrer S, Comin F. Separation of the $sp^2$and sp^3 components in the C1s photoemission spectra of amorphous carbon films. Phys Rev B 1996;54(11):8064–9.
[43] Schelz R, Richmond T, Kania P, Oelhafen P, Güntherodt H-J. Electronic and atomic structure of evaporated carbon films. Surf Sci 1996;359:227–36.
[44] Butenko YuV, Krishnamurthy S, Chakraborty AK, Kuznetsov VL, Dhanak VR, Hunt MRC, et al. Photoemission study of onionlike carbons produced by annealing nanodiamonds. Phys Rev B 2005;71(10):075420-1–075420-10.